

SUPPLEMENTARY INFORMATION GUIDE

Tumour DDR1 Promotes Collagen Fibre Alignment to Instigate Immune Exclusion

Xiujie Sun^{1#}, Bogang Wu^{1#}, Huai-Chin Chiang^{1#}, Hui Deng², Xiaowen Zhang¹, Wei Xiong², Junquan Liu², Aaron M. Rozeboom³, Brent Harris³, Eline Blommaert⁴, Antonio Gomez⁵, Roderic Espin Garcia⁴, Yufan Zhou⁶, Payal Mitra⁷, Madeleine Prevost¹, Deyi Zhang⁸, Debarati Banik¹, Claudine Isaacs³, Deborah Berry³, Catherine Lai³, Krysta Chaldekas³, Patricia S. Latham⁹, Christine A. Brantner¹⁰, Anastas Popratiloff¹⁰, Victor X. Jin⁶, Ningyan Zhang², Yanfen Hu⁷, Miguel Angel Pujana^{4*}, Tyler J. Curiel^{8*}, Zhiqiang An^{2*}, Rong Li^{1*}

¹Department of Biochemistry & Molecular Medicine,

⁷Department of Anatomy & Cell Biology, ⁹Department of Pathology,

School of Medicine & Health Sciences,

¹⁰GW Nanofabrication and Imaging Center,

The George Washington University, Washington, DC 20037, USA

²Texas Therapeutics Institute, Brown Foundation Institute of Molecular Medicine,

The University of Texas Health Science Center at Houston, Houston, TX 77030, USA

³Lombardi Comprehensive Cancer Center,

Georgetown University, Washington, DC 20007, USA

⁴ProCURE, Catalan Institute of Oncology, Oncobell, Bellvitge Institute for Biomedical

Research (IDIBELL), L'Hospitalet del Llobregat, Barcelona, Catalonia, Spain

⁵Rheumatology Department and Rheumatology Research Group, Vall d'Hebron Hospital

Research Institute, Barcelona, Spain

⁶Department of Molecular Medicine, ⁸Department of Medicine, The Mays Cancer Center,

University of Texas Health San Antonio, San Antonio, TX 78229, USA

Running Title: Breaking down DDR1-dependent immune exclusion

#These authors contributed equally to the work

*Correspondence to: R.L. (rli69@gwu.edu), Z.A. (Zhiqiang.An@uth.tmc.edu), T.J.C. (curielt@uthscsa.edu), M.A.P. (mapujana@iconcologia.net)

Table of Contents

Supplementary Figure 1. Gel source data for Main Figure 1a. (Page 1)

Supplementary Figure 2. Gel source data for Extended Figure 1a. (Page 2)

Supplementary Figure 3. Representative gating strategies for flow cytometry analysis of TILs used in this study. (Page 3)

Supplementary Figure 4. Immune- related transcriptomic changes. (Page 4-5)

Supplementary Figure 5. PCA of transcriptome profiles across studies and samples. (Page 6-7)

Supplementary Figure 6. DEGs between *Ddr1*-KO and WT tumours/cells. (Page 8-9)

Supplementary Figure 7. Profiles of DEGs from immunocompetent host tumours and GO annotations. (Page 10-11)

Supplementary Figure 8. Gel source data for Extended Data Figure 5c. (Page 12)

Supplementary Figure 9. Gel source data for Extended Data Figure 5d. (Page 13)

Supplementary Figure 10. Gel source data for Extended Data Figure 5g. (Page 14)

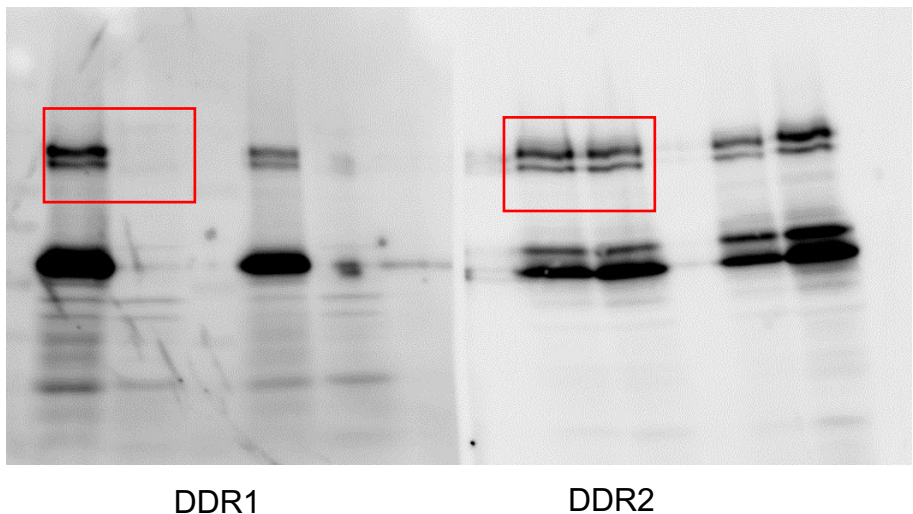
Supplementary Figure 11. Gel source data for Extended Data Figure 5h. (Page 15)

Supplementary Figure 12. Gel source data for Extended Data Figure 5i. (Page 16)

Supplementary Figure 13. Gel source data for Extended Data Figure 7a. (Page 17)

Supplementary Figure 14. GO analysis of DEGs from RNA-seq of E0771 KO+huDDR1 tumours, treated with control IgG and anti-DDR1 antibody (#9) (n=4 each group; harvested on day 6 after antibody administration). (Page 18)

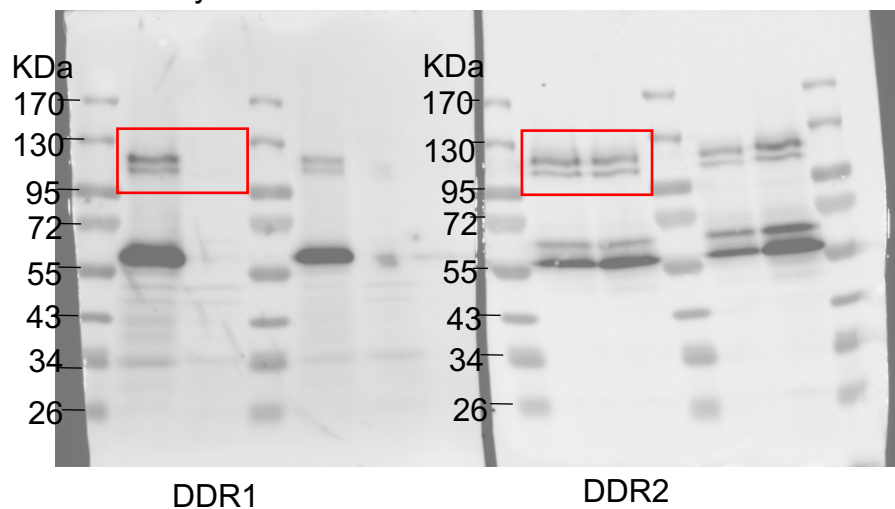
Supplementary Figure 1. Gel source data for Main Figure 1a



DDR1

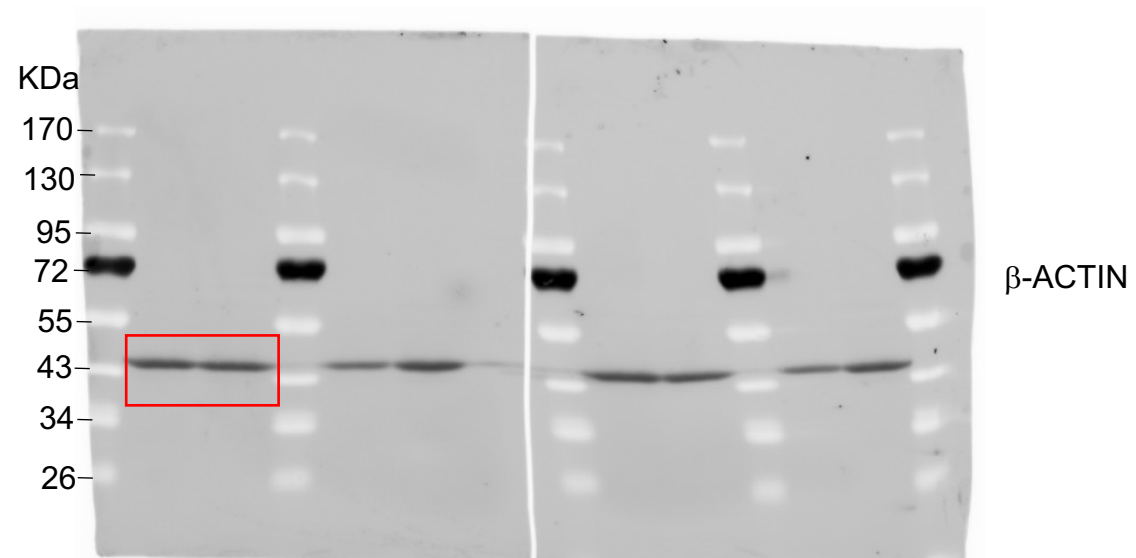
DDR2

Overlay with marker

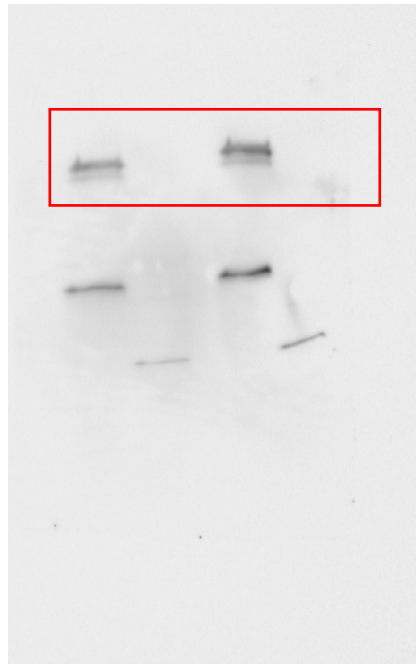


DDR1

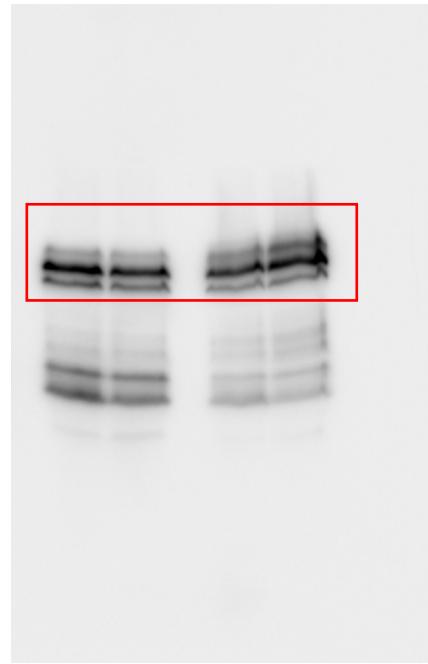
DDR2



Supplementary Figure 2. Gel source data for Extended Data Figure 1a

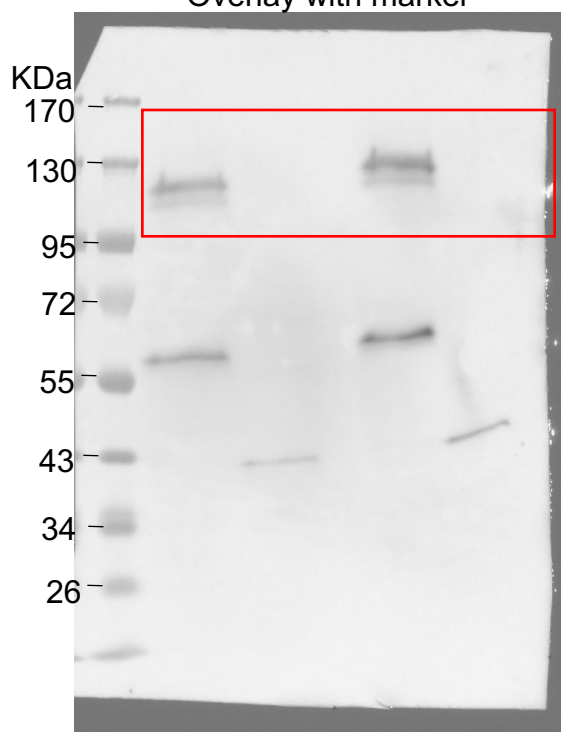


DDR1

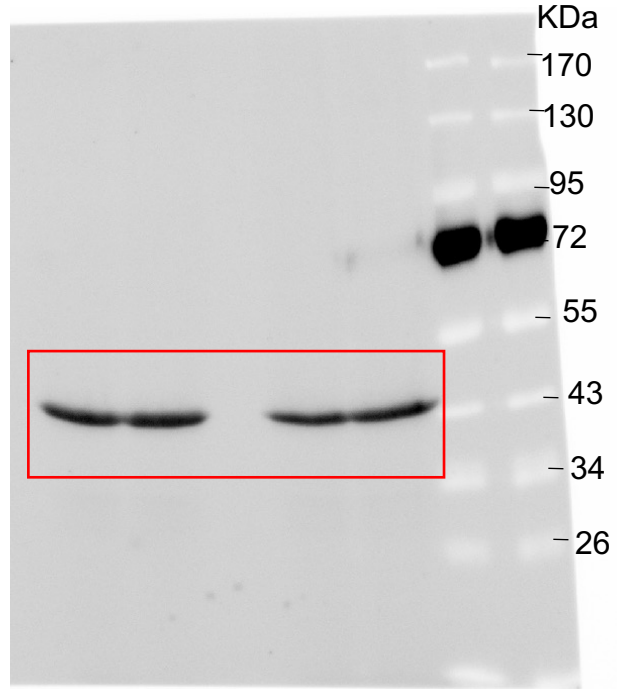


DDR2

Overlay with marker

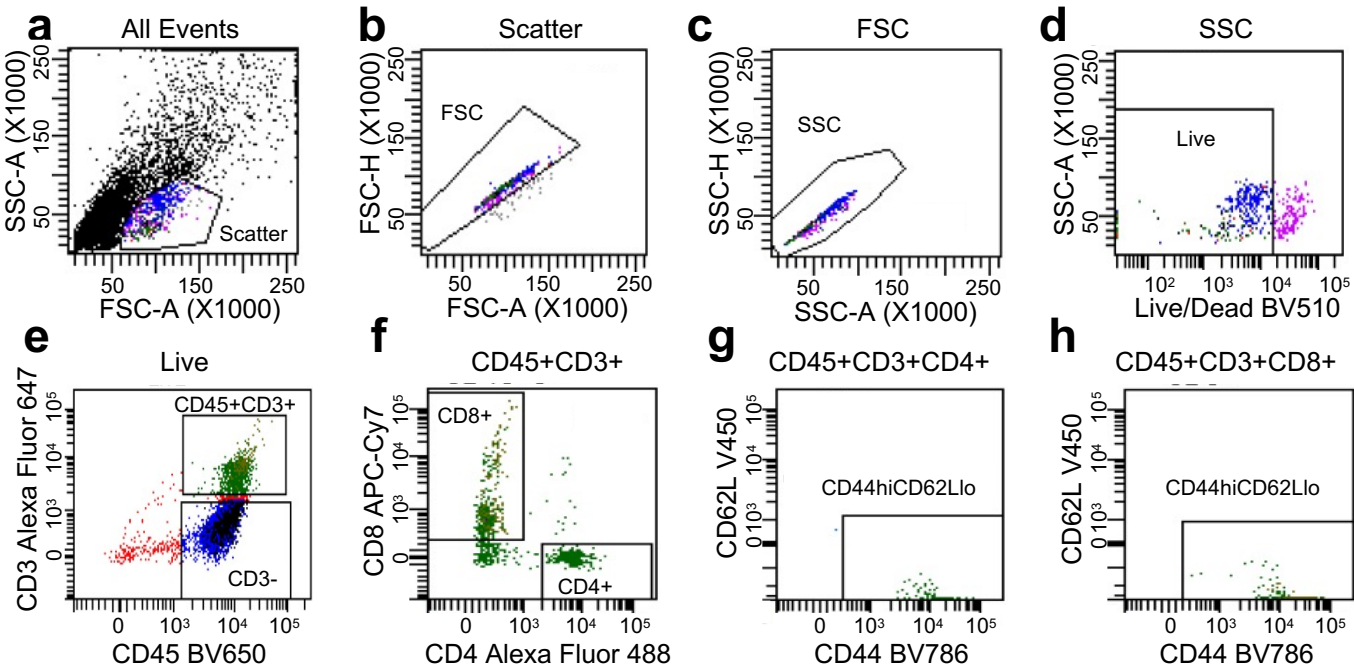


DDR1



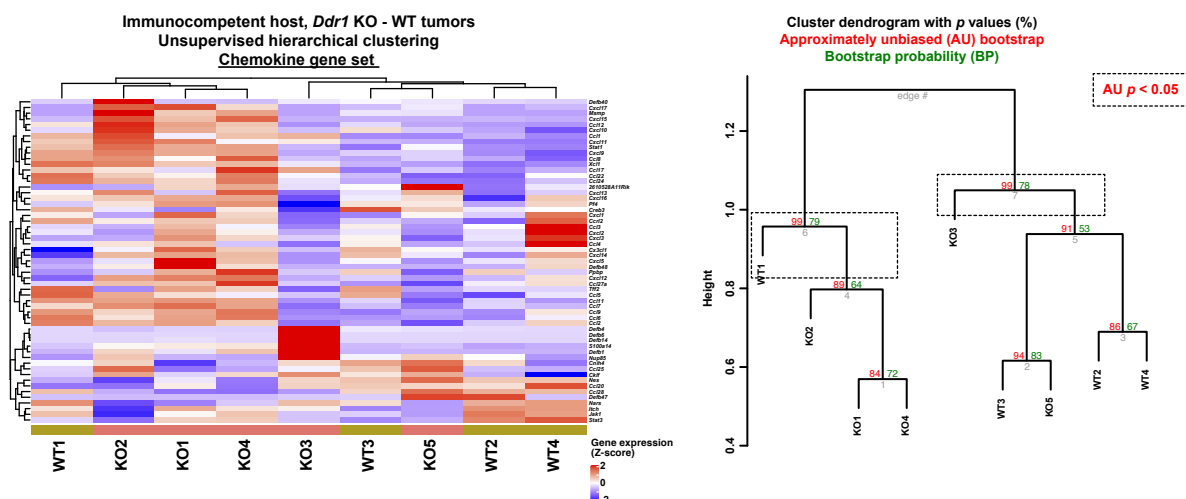
β -ACTIN

Supplementary Figure 3. Representative gating strategies for flow cytometry analysis of TILs used in this study.

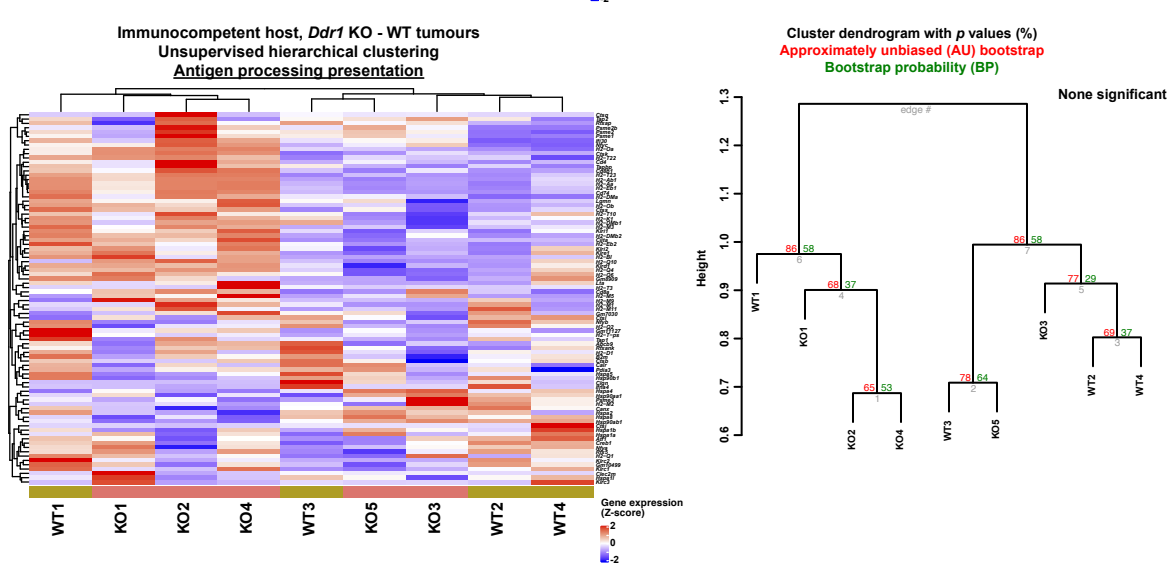


Supplementary Figure 4. Immune-related transcriptomic changes

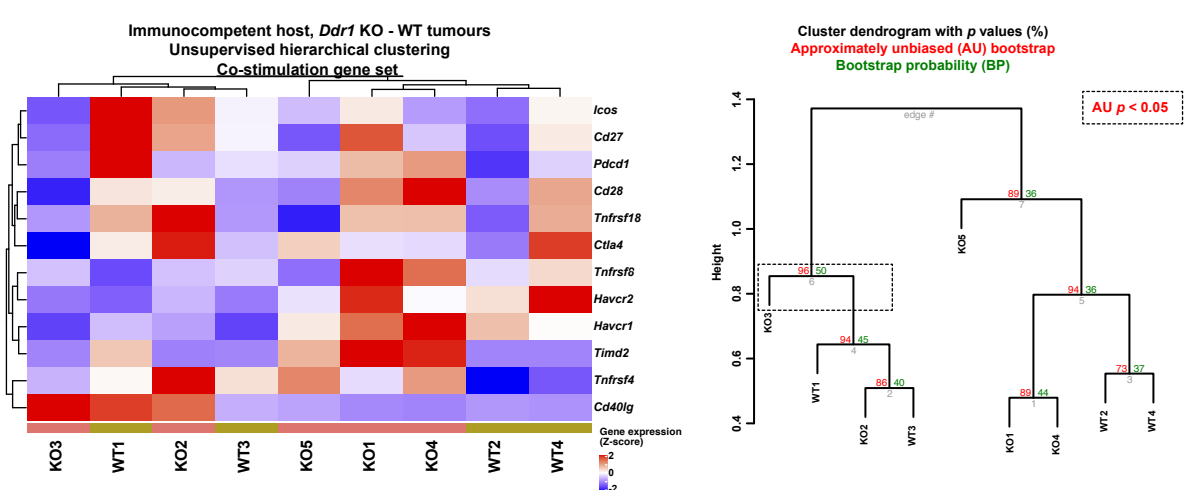
a



b



c

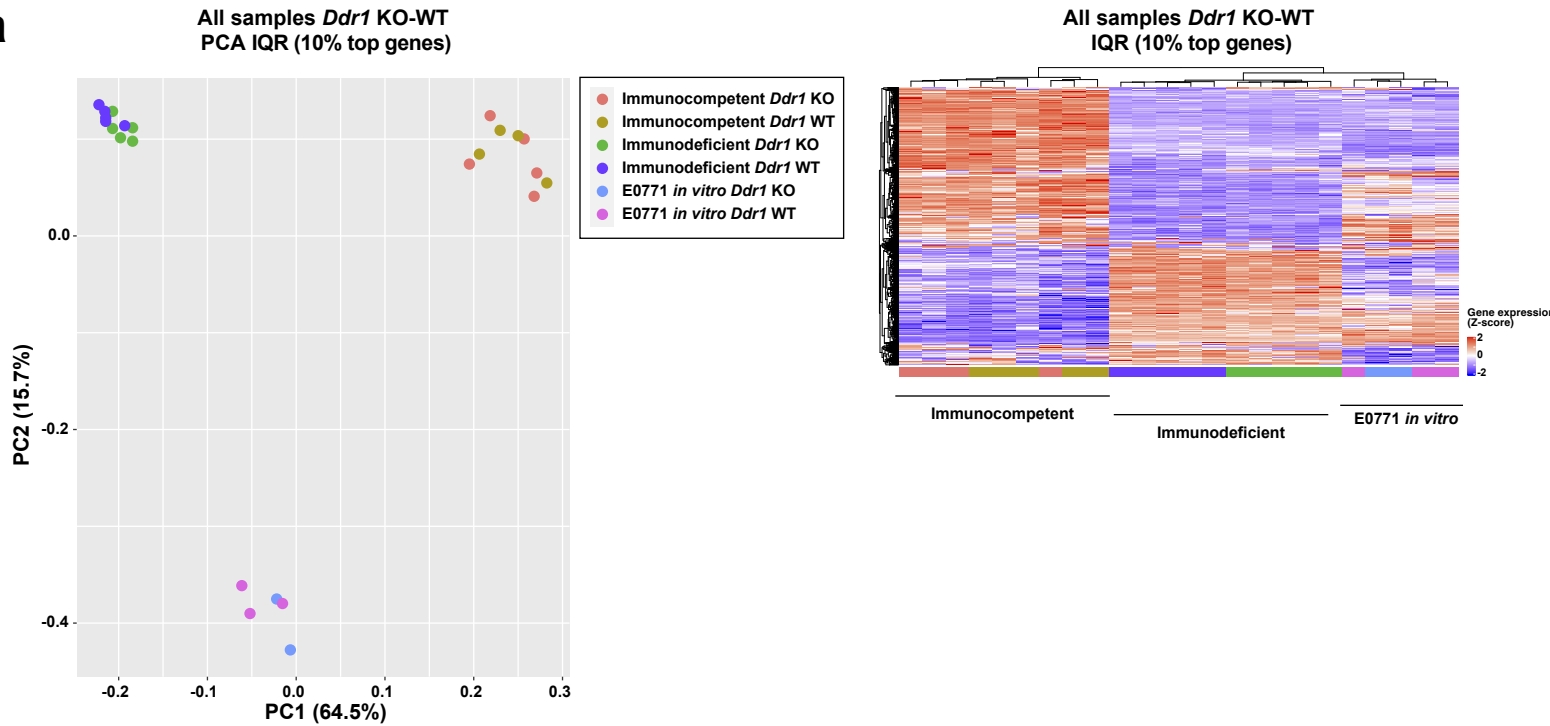


Supplementary Figure 4. Immune-related transcriptomic changes.

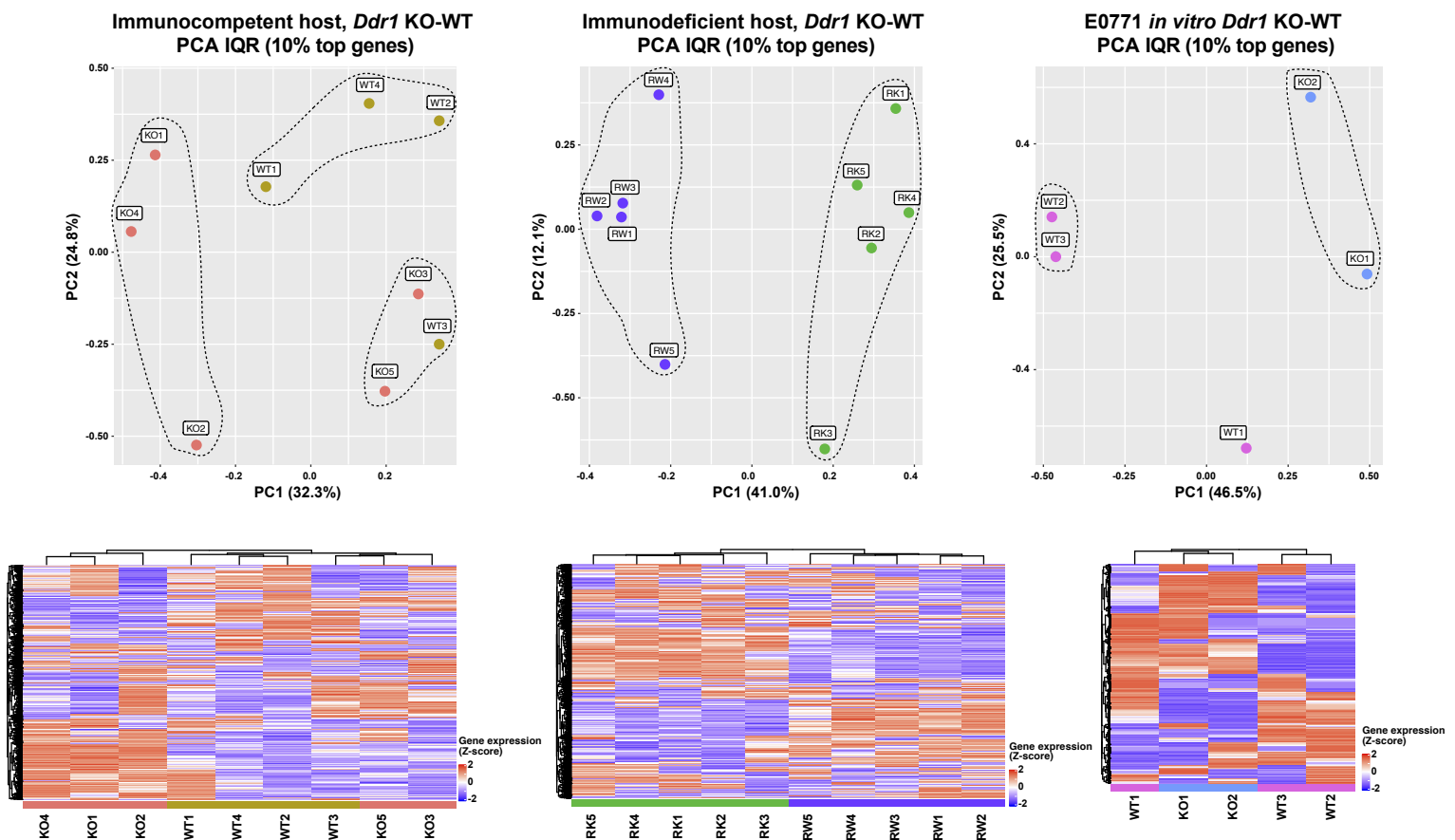
(a-c) Left panels, unsupervised hierarchical clustering of the expression of immune-related gene sets in *Ddr1*-WT and KO tumours from immunocompetent hosts: chemokine genes (a); genes involved in antigen processing/presentation (b); and co-stimulation genes (c). Right panels, hierarchical clustering performed for the gene sets using the R package Pvclust. Values at branches are approximately unbiased (AU) *p* values (left, red font) and bootstrap probability (BP) values (right, green font). The clusters considered significant (AU *p* < 0.05) are marked by dashed rectangles.

Supplementary Figure 5. PCA of transcriptome profiles across studies and samples

a



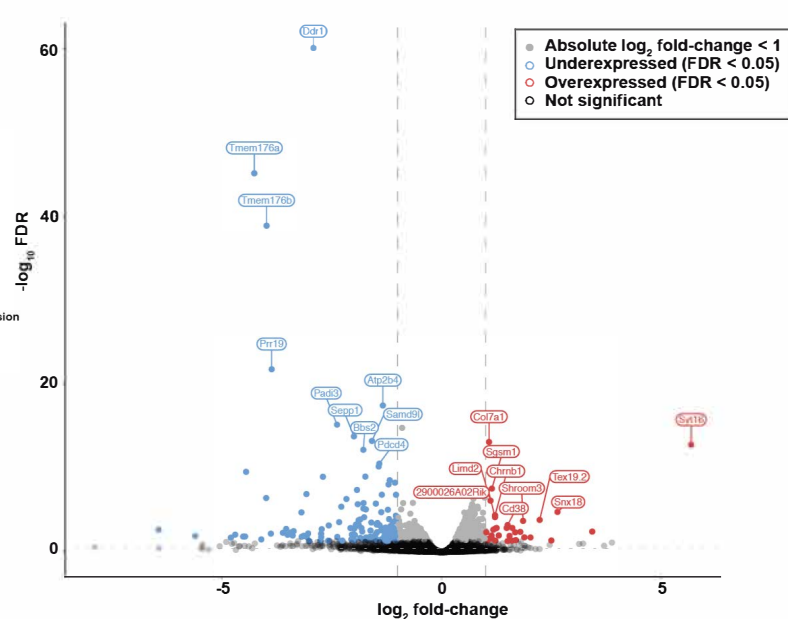
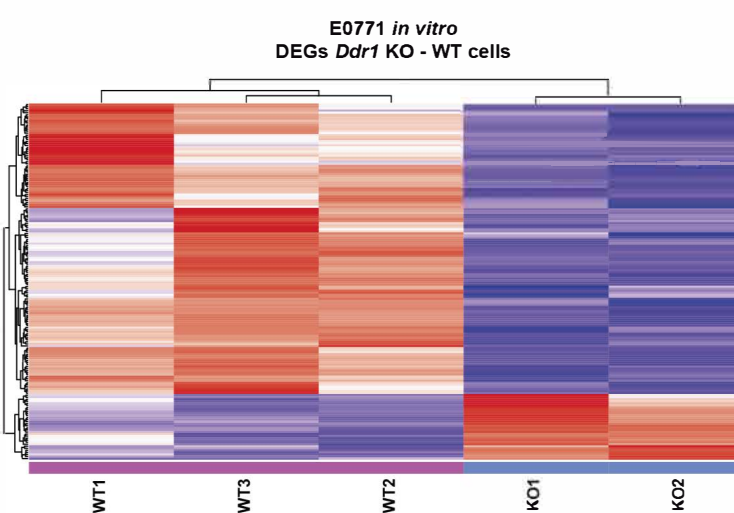
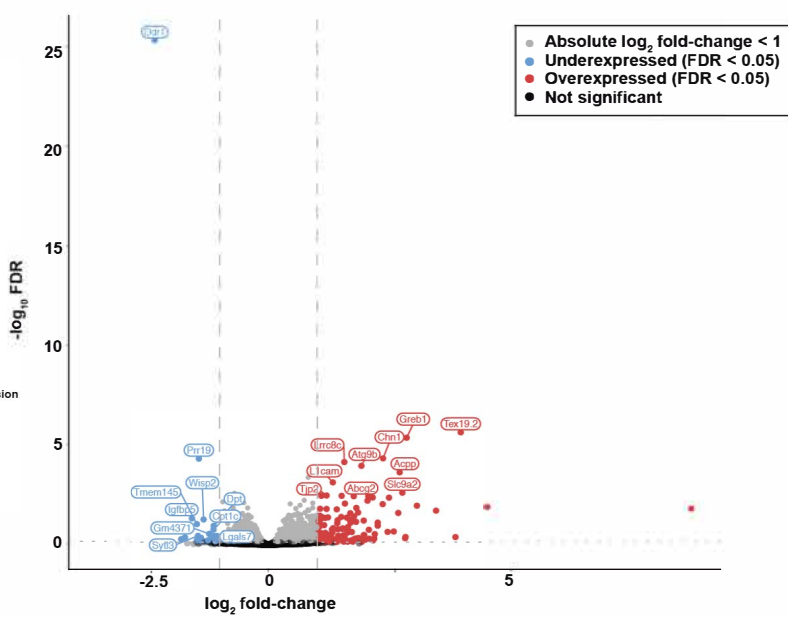
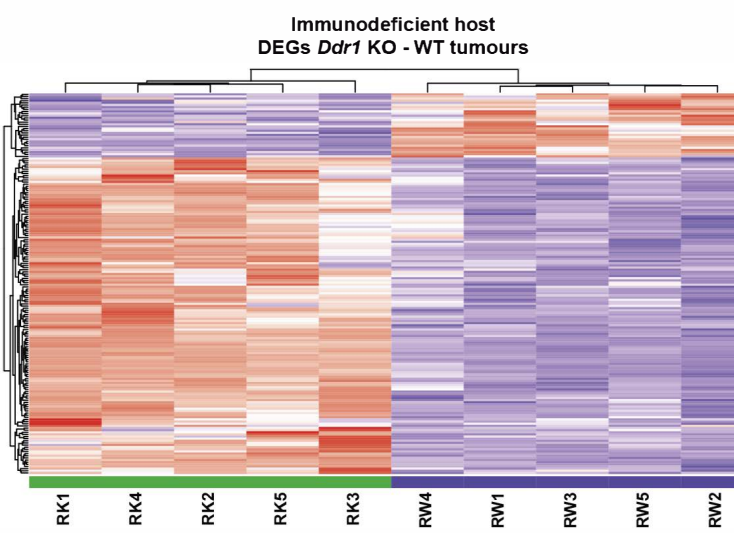
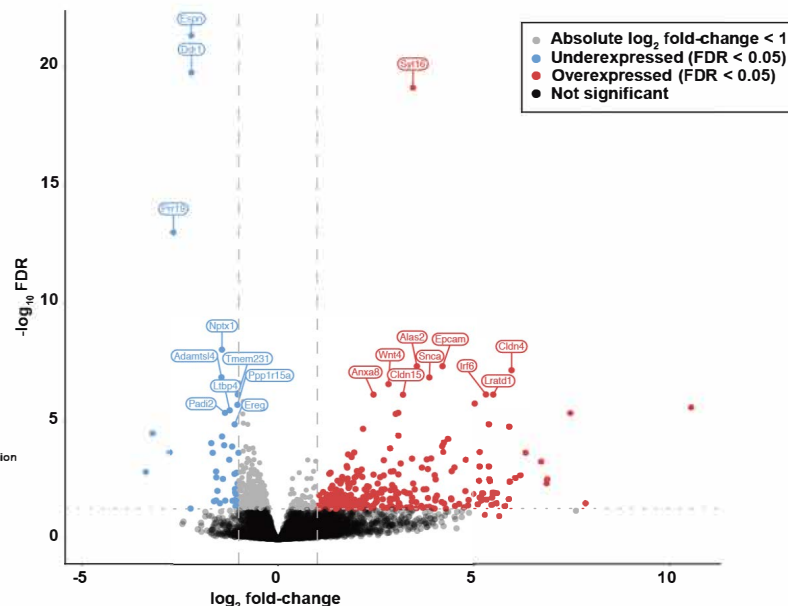
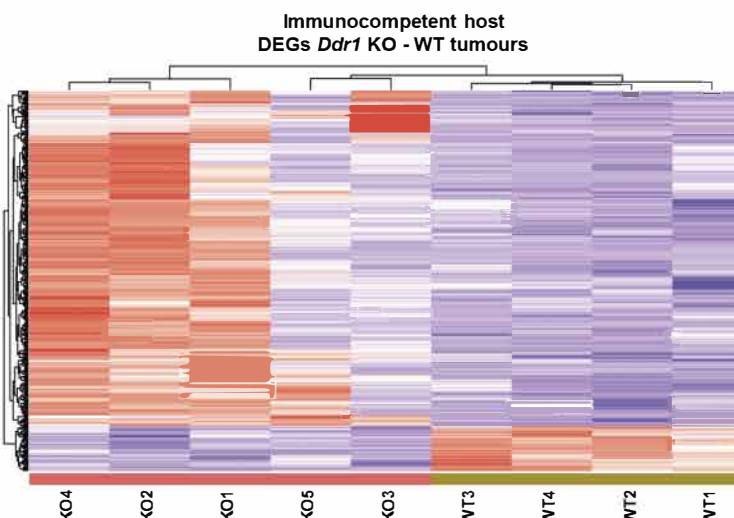
b



Supplementary Figure 5. PCA of transcriptome profiles across studies and samples. (a)

Left panel, PCA plot including all tumours/cells analysed by RNA-seq. Right panel, unsupervised hierarchical clustering of the genes with the highest (10% top) IQR. The gene list is provided in Extended Data Table 1. **(b)** Top panels, PCA plots of the tumours/cells analysed by RNA-seq in each setting. Bottom panels, unsupervised hierarchical clustering of the genes with the highest (10% top) IQR in each setting. The gene lists are provided in Supplementary Table 1.

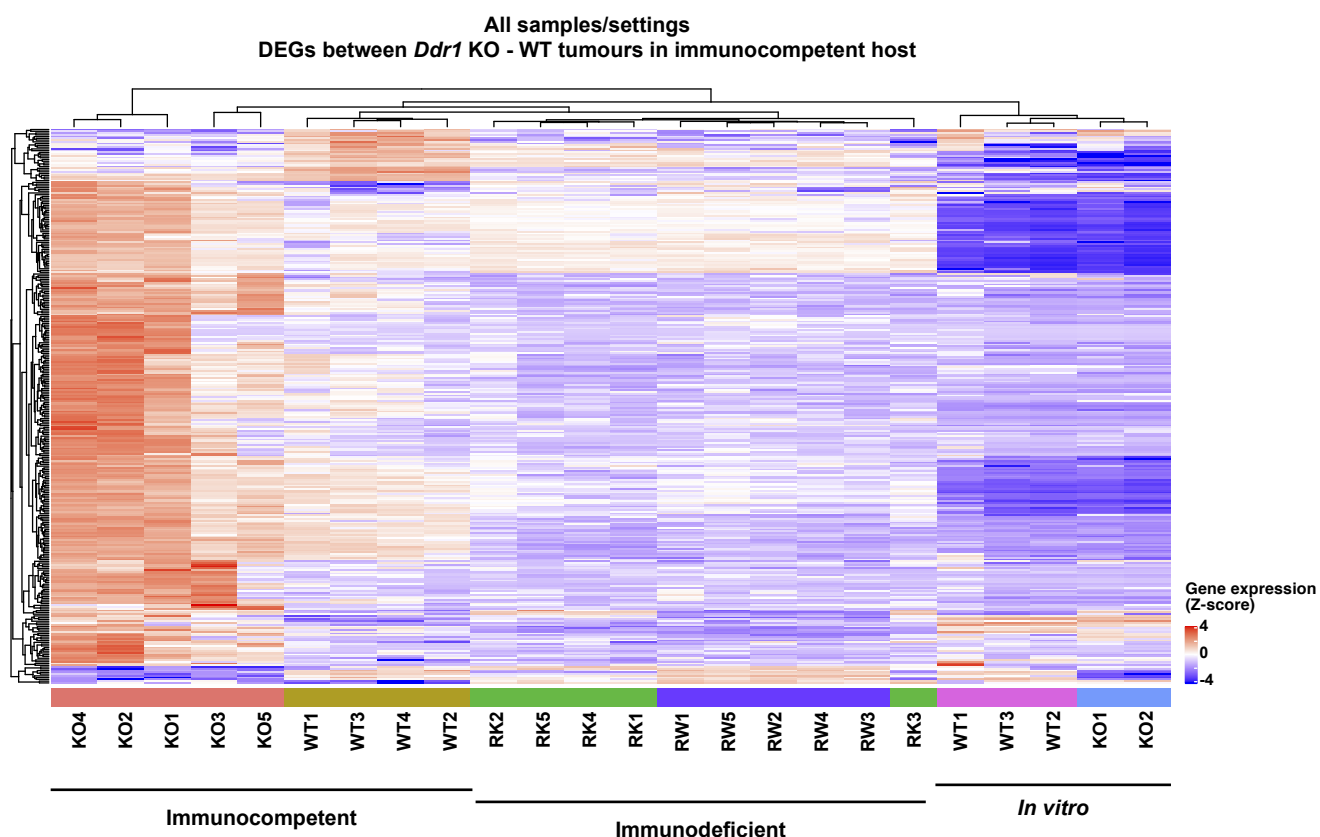
Supplementary Figure 6. DEGs between *Ddr1*-KO and WT tumours/cells



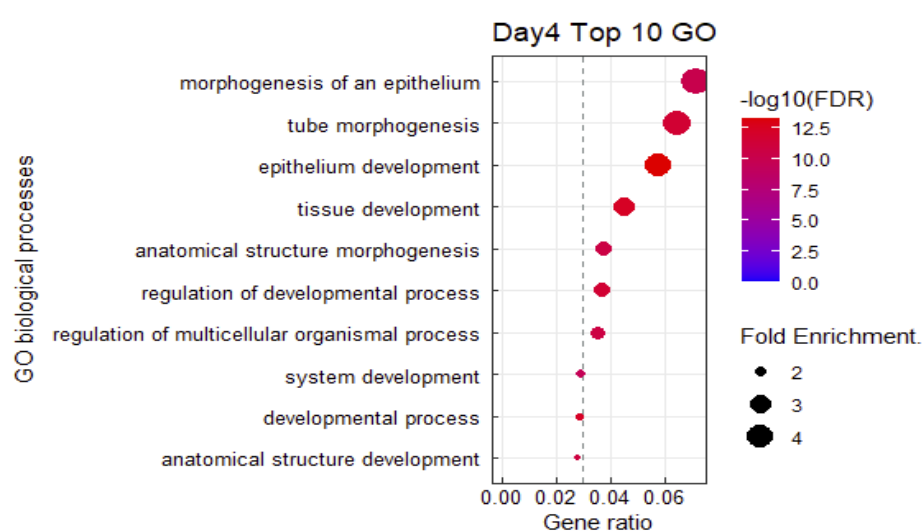
Supplementary Figure 6. DEGs between *Ddr1*-KO and WT tumours/cells. Left panels, unsupervised hierarchical clustering of DEGs (FDR-adjusted $p < 0.05$) in each setting (top, immunocompetent host; middle, immunodeficient host; bottom, E0771 cells *in vitro*). Right panels, Volcano plots of differential gene expression between *Ddr1*-KO and WT tumours/cells. Genes are plotted in different colours depending on their significance and absolute \log_2 fold-change (inset). The names of the 10-top differentially expressed genes in each direction and setting are indicated. The complete lists of DEGs are provided in Supplementary Table 2.

Supplementary Figure 7. Profiles of DEGs from immunocompetent host tumours and GO annotations

a



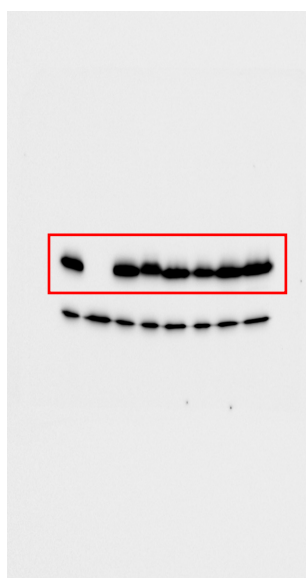
b



Supplementary Figure 7. Profiles of DEGs from immunocompetent host tumours and GO annotations. (a) Unsupervised hierarchical clustering of all settings/samples using DEGs identified in the comparison between *Ddr1*-KO and WT tumours developed in immunocompetent host. (b) GO analysis of immunocompetent host-unique DEGs.

Supplementary Figure 8. Gel source data for Extended Data Figure 5c

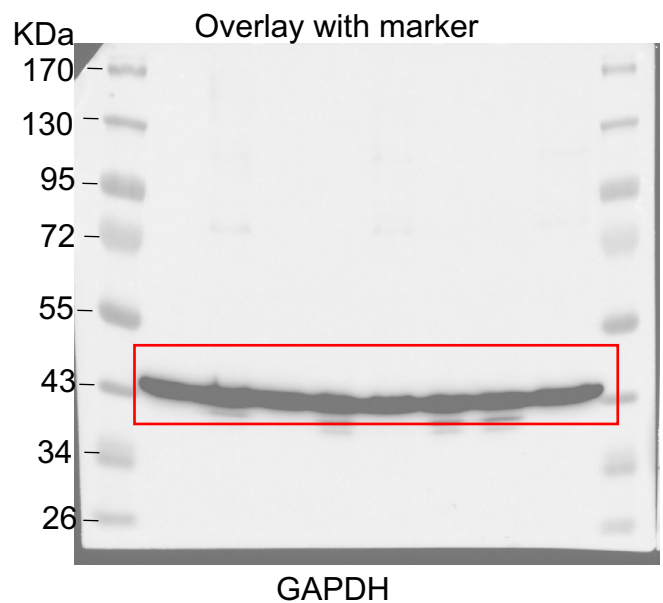
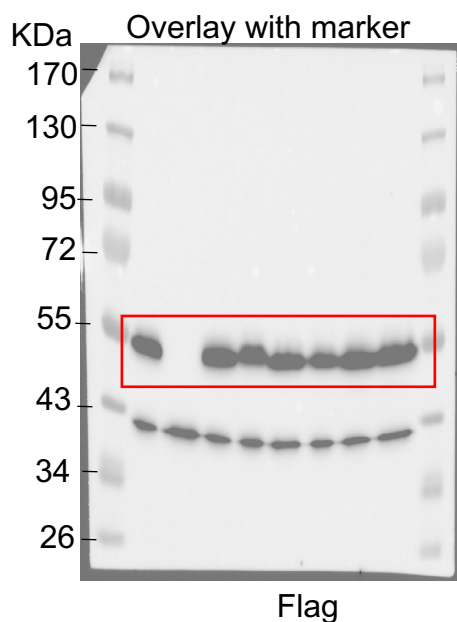
M-Wnt



Flag

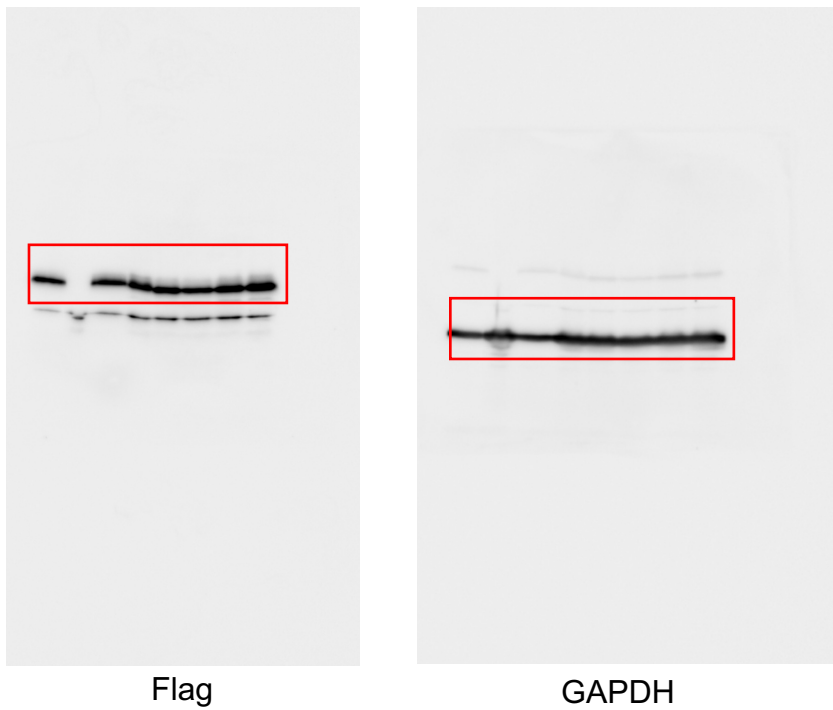


GAPDH



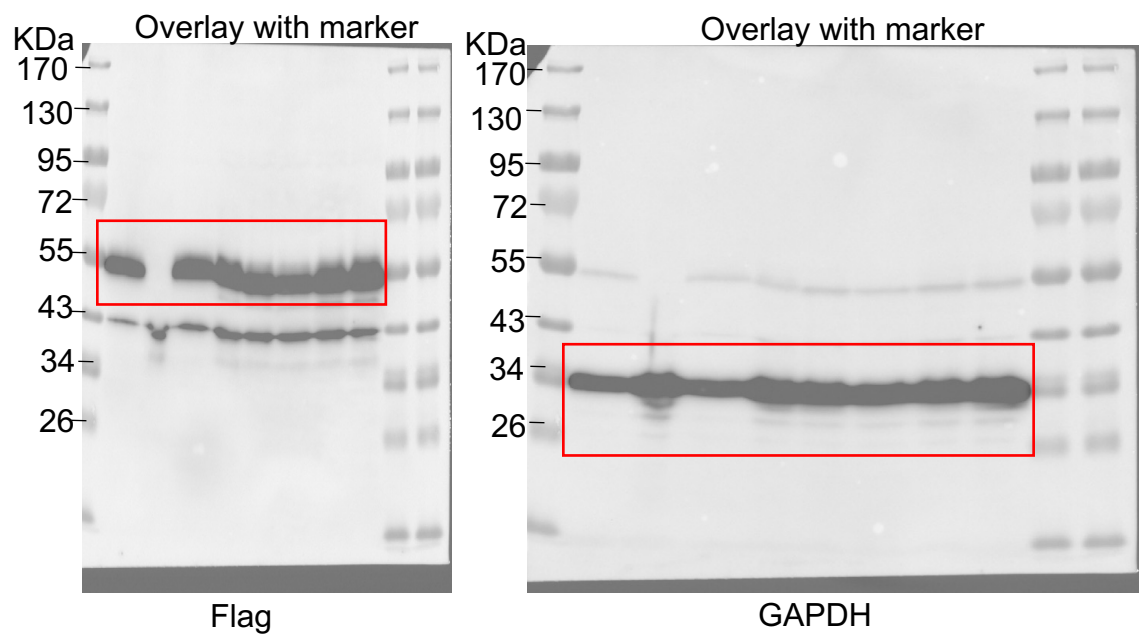
Supplementary Figure 9. Gel source data for Extended Data Figure 5d

AT-3



Flag

GAPDH

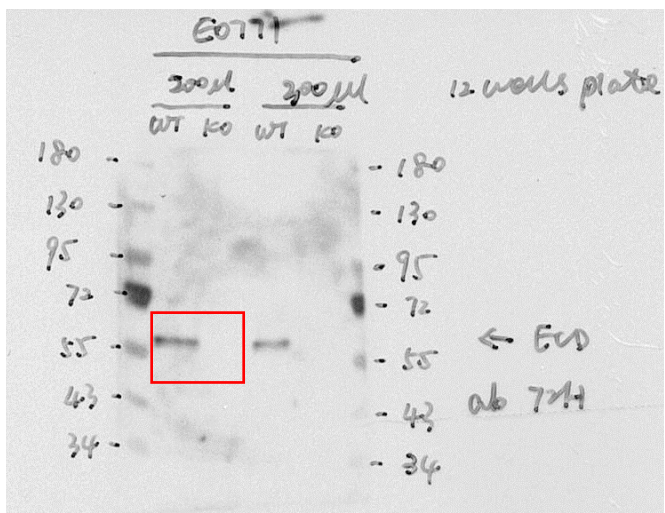


Flag

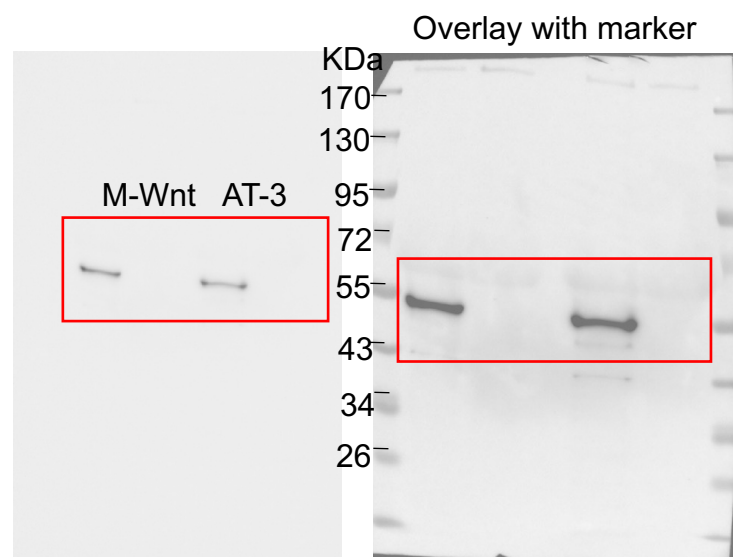
GAPDH

Supplementary Figure 10. Gel source data for Extended Data Figure 5g

Conditioned Medium:

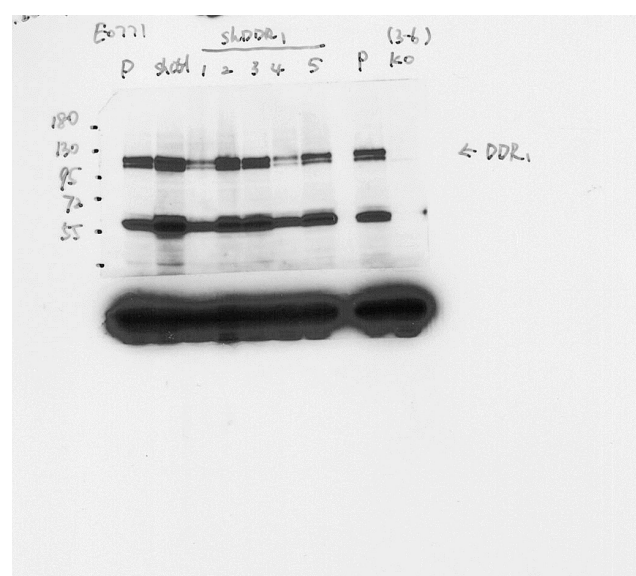


DDR1 ECD



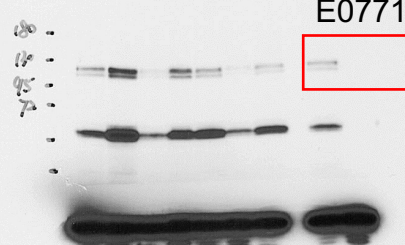
DDR1 ECD

Overlay with marker

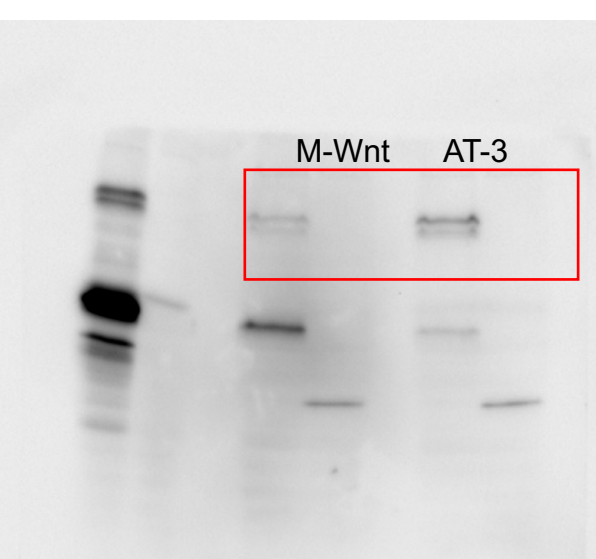


—

E0771

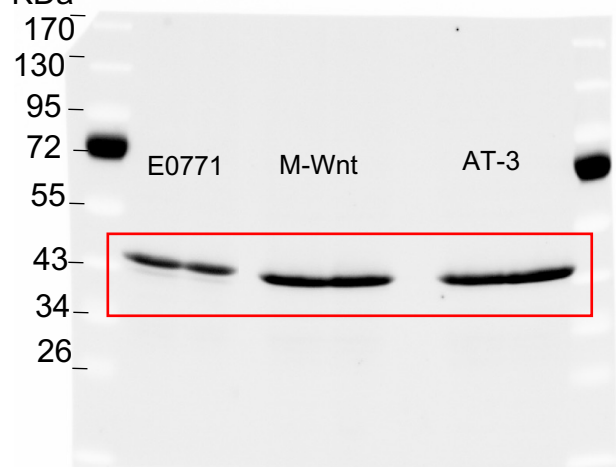


FL DDR1



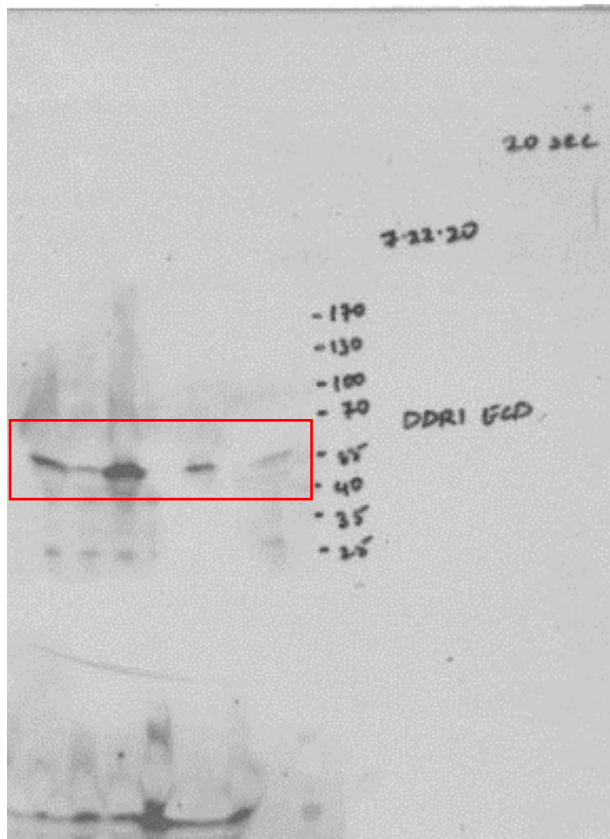
FL DDR1

KDa



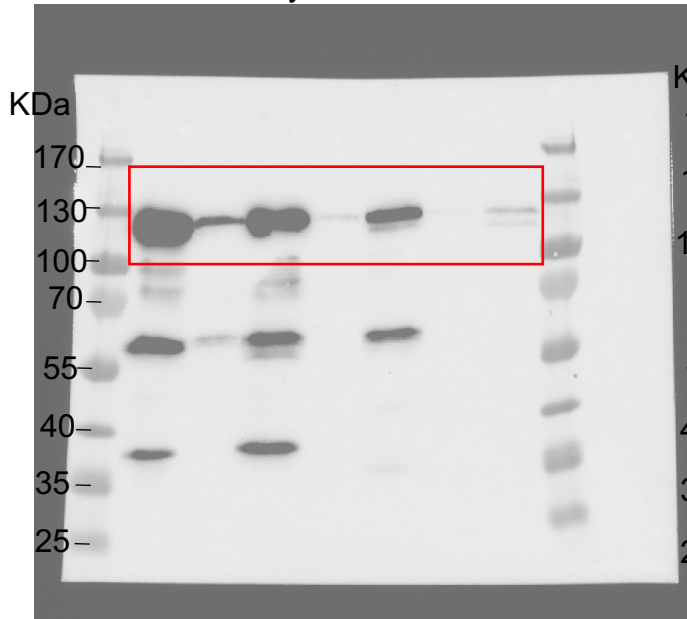
Supplementary Figure 11. Gel source data for Extended Data Figure 5h

Conditioned Medium



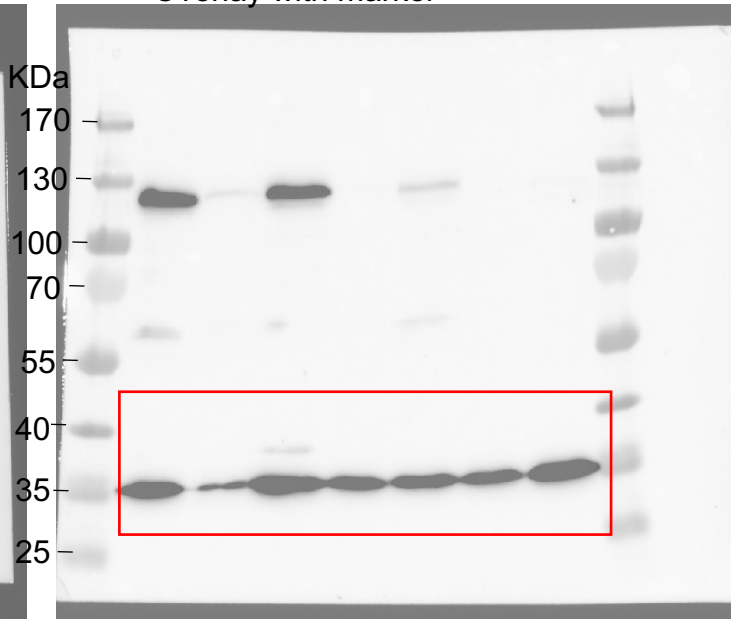
DDR1 ECD

Overlay with marker



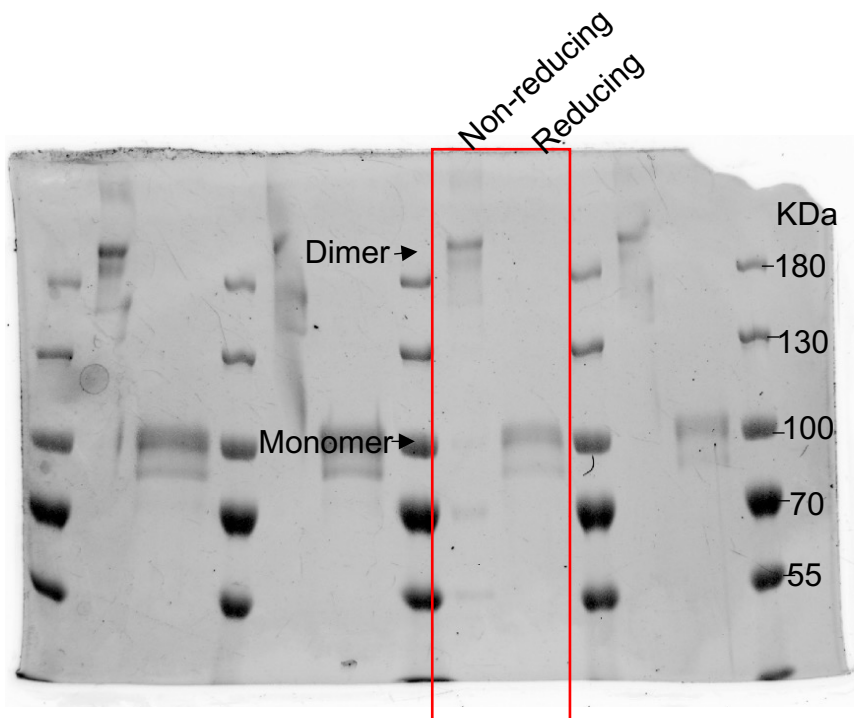
FL DDR1

Overlay with marker



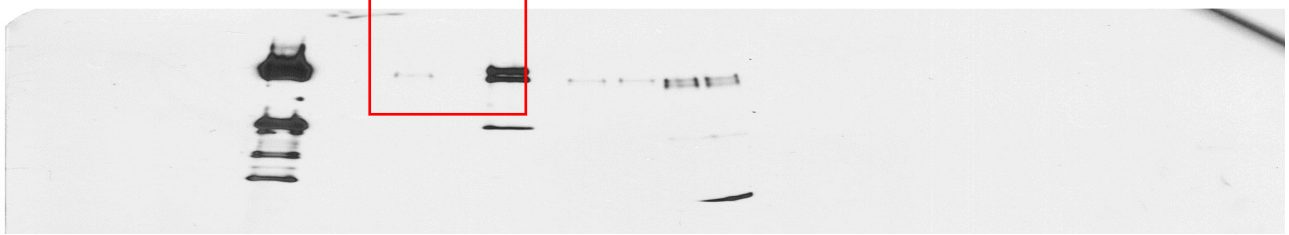
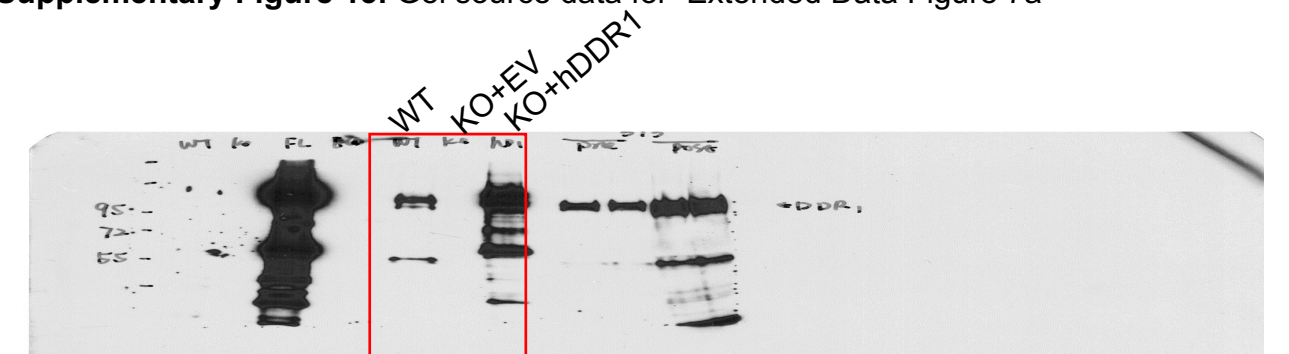
GAPDH (probed after stripping)

Supplementary Figure 12. Gel source data for Extended Data Figure 5i

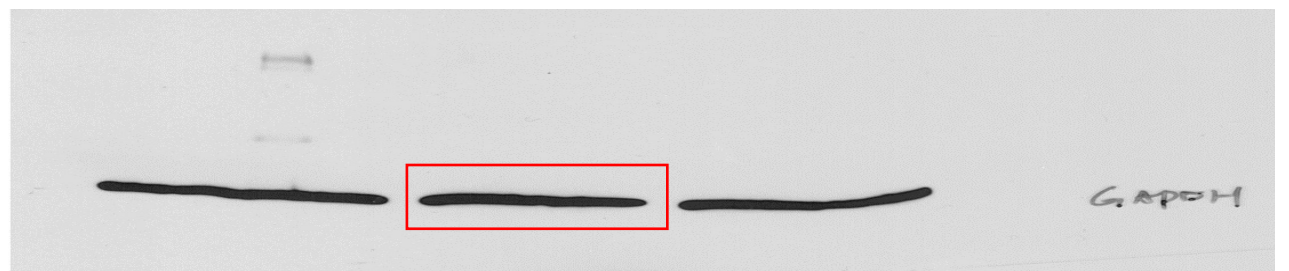


Coomassie Gel Staining

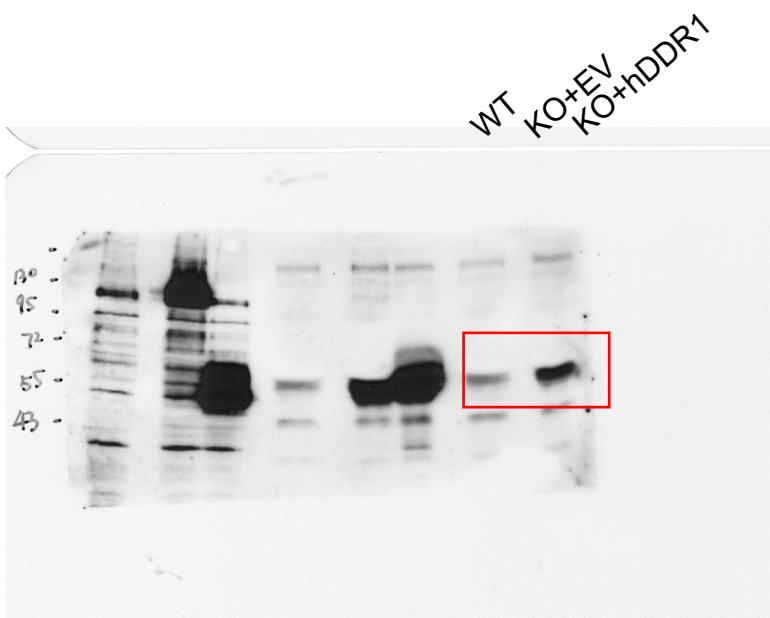
Supplementary Figure 13. Gel source data for Extended Data Figure 7a



FL DDR1



GAPDH



DDR1 ECD

Supplementary Figure 14. GO analysis of DEGs from RNA-seq of E0771 KO+huDDR1 tumours, treated with control IgG and anti-DDR1 antibody (#9) ($n=4$ each group; harvested on day 6 after antibody administration).

